A&A 369, L9–L12 (2001)
DOI: 10.1051/0004-6361:20010219

Astronomy & Astrophysics

Pyramid Wavefront Sensor behavior in partial correction Adaptive Optic systems

S. Esposito and A. Riccardi

Osservatorio Astrofisico di Arcetri, Largo E. Fermi 5, 50125 Firenze, Italy

Received 20 November 2000 / Accepted 7 February 2001

Abstract. In this letter we evaluate the limiting magnitude for a Pyramid Sensor operating in a closed loop astronomical Adaptive Optics system. A first heuristic analysis has shown that, when a point-like reference source is used a pyramid sensor exhibits a significant gain in terms of limiting magnitude over the widely used Shack-Hartmann sensor. This when diffraction limited conditions are reached. However, in current astronomical Adaptive Optics, diffraction limited regime at the sensing wavelength is difficult to achieve. Our simulations quantify the pyramid sensor limiting magnitude considering an Adaptive Optics system working in a partial correction regime. The simulations show that the considered gain is retained even in partial correction. An average gain of two magnitude is found in the considered case. This feature of a pyramid sensor can be very important in reducing the fundamental limit of today's Astronomical Adaptive Optics systems using natural reference sources, i.e. the limited sky-coverage.

Key words. atmospheric effects – instrumentation: adaptive optics

1. Introduction

This letter reports the results of computer simulations aimed at evaluating the Pyramid Sensor (Ragazzoni 1996) (PS) behavior in partial correction Adaptive Optics (AO) systems. It has been heuristically demonstrated that when diffraction limited correction is approached at the sensing wavelength, a PS performs better then a Shack-Hartmann sensor (SHS) in terms of limiting magnitude (Ragazzoni & Farinato 1999). This is because in diffraction limited conditions the SHS sensitivity is limited by diffraction effects introduced by the sensing subapertures, while PS sensitivity is limited by diffraction effects introduced by the whole telescope aperture. The above statement holds when a point-like reference source is used. However, diffraction limited correction is difficult to reach at the sensing wavelength with the present generation of AO systems. For this reason our numerical code simulates PS and SHS behavior in partial correction regime using diffractive optics to evaluate the gain in limiting magnitude as a function of the AO system correction efficiency.

Section 2 briefly describes the sensor optical configuration and reports the equations that relate the PS signals to the wavefront perturbations. Section 3 outlines the numerical simulations of the sensor in closed loop operation (Esposito et al. 2000). Section 4 considers the 6.5 m MMT telescope to show the different behavior of PS and SHS. In Sects. 4.1 and 4.2 reconstruction error and limiting magnitude for PS and SHS are calculated and compared respectively.

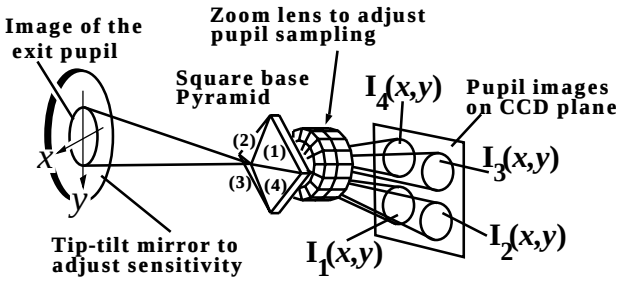

Fig. 1. A sketch of the pyramid sensor optical set-up. The tip-tilt mirror con be substituted with a translation stage that translates the pyramid in the focal plane

2. PS principle of operation

The basic configuration of the PS is shown in Fig. 1. It consists of three fundamental parts: a tip-tilt mirror conjugated to the exit pupil of the system under test, a square-based glass pyramid with its vertex at the nominal focal plane of the system and a relay lens that forms four images of the exit pupil on a CCD detector. When the tip-tilt mirror is not oscillating, the configuration is fully equivalent

Send offprint requests to: S. Esposito,
e-mail: esposito@arcetri.astro.it

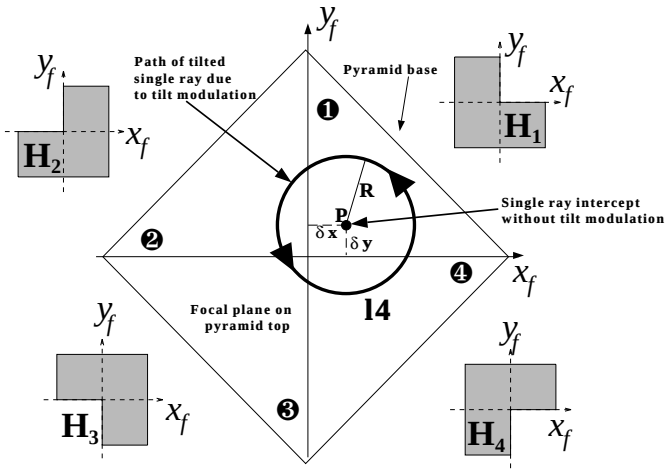

Fig. 2. Effect of tilt modulation in the PS focal plane

to a Foucault (Foucault 1859) knife-edge test (Babcock 1953; Horwitz 1994; Gale Wilson 1975). However, in the considered configuration (Ragazzoni 1996), information on the X and Y derivatives can be collected simultaneously. Introducing a periodic modulation of the wavefront tilt (e.g. a circular one using the tip-tilt mirror Santagata) allows the sensor sensitivity to be changed[1]. PS sensitivity is found to be inversely proportional to the tip-tilt modulation amplitude. This allows the PS sensitivity to be adjusted in order to deal with different amplitudes of the incoming wavefront aberration. In closed loop operation, the sensitivity can be increased as the wavefront correction progresses, as is usually done in the case of curvature sensing systems (Roddier 1990; Roddier et al. 1991). In the case of a circular tip-tilt modulation having amplitude bigger than the local tilt of the aberrated wavefront $w(x,y)$, geometrical optics calculations show that (Esposito et al. 1999; Riccardi et al. 1998):

$$\frac{\partial w}{\partial x}(x,y) = \frac{R}{F}\sin\left(\frac{\pi}{2}S_x(x,y)/\sum_{i=1}^{4} I_i(x,y)\right), \quad (1)$$

where, referring to Figs. 1 and 2, F is the linear distance between the system exit pupil (located on the tip-tilt mirror) and the nominal focal plane, R is the linear tip-tilt modulation amplitude on the focal plane and $I_i(x,y)$ are the intensity distribution in the ith pupil image obtained by the PS. Furthermore S_x is the sensor signal defined as

$$S_x(x,y) = [I_1(x,y) + I_4(x,y)] - [I_2(x,y) + I_3(x,y)]\,. \quad (2)$$

Similar equations hold for $\partial w/\partial y$ and S_y. In the case of a generic tip-tilt modulation and wavefront aberration amplitude, diffraction theory can be used to find the relationship between the wavefront phase aberrations $\phi(x,y) = 2\pi w(x,y)/\lambda$ and the sensor signals. It can be shown that (Riccardi & Esposito, in preparation), for a square-based pyramid, the signals S_x and S_y depend on integrals of functions containing $\phi(x,y)$ and the tilt amplitude of the form

$$\sin\left[\phi(P_1) - \phi(P_2)\right] \mathrm{J}_0\left(kd_{12}R/F\right), \quad (3)$$

where $k = 2\pi/\lambda$, J_0 is the zeroth order Bessel function, P_1 and P_2 are two generic points on the pupil and d_{12} is the distance between them. In the case of small aberrations, such as those encountered in closed loop AO applications, we have

$$\sin\left[\phi(P_1) - \phi(P_2)\right] \approx \phi(P_1) - \phi(P_2). \quad (4)$$

With this approximation the sensor signals are obtained as a linear combination of the phase perturbations. This permits the use of linear systems theory to describe sensor operation.

3. Partial correction AO system and PS behavior

The principal aim of the simulation is to evaluate the limiting magnitude of a PS working in a closed loop AO system. This translates directly into calculating the reconstruction error σ^2_{rec} as a function of the phase variance of the wavefront corrected by the AO system σ^2_{c}, for a given number of detected photons. Both variances σ^2_{rec} and σ^2_{c} are evaluated at the sensing wavelength. An unavoidable part of the PS reconstruction error is due to the non linearity of Eq. (3). Moreover the simulation takes into account reconstruction error due to photon noise. To quantify the overall reconstruction error a diffractive calculation of the sensor signals is performed and the wavefront is reconstructed using a standard least-square modal reconstructor. Sensing and reconstruction processes are repeated for a set of Montecarlo generated wavefronts. These wavefronts are generated as linear combination of Zernike polynomials using a standard algorithm for atmospherically perturbed wavefronts (Roddier 1990b). To simulate sensor operation in a partial correction regime the Zernike coefficients of the various sets of realizations are attenuated to obtain different values of the partially corrected wavefront variance σ^2_{c}. The main part of the simulation routines is devoted to calculation of the pupil image illumination patterns generated by a certain incoming wavefront. According to diffraction theory it can be shown (Gale Wilson 1975) that the intensity distribution of the four pupil images $I_i(x,y)$ is given by

$$I_i(x,y) \propto \left|\mathrm{FT}^{-1}\left[H_i(x_{\mathrm{f}},y_{\mathrm{f}})\mathrm{FT}\left[P(x,y)\exp(i\phi(x,y))\right]\right]\right|^2, \quad (5)$$

where the functions $H_i(x_{\mathrm{f}},y_{\mathrm{f}})$ $(i = 1,2,3,4)$ account for the spatial filter effect introduced by the ith pyramid facet in the focal plane (see Fig. 2), $P(x,y)$ is the system pupil function and FT is the Fourier Transform operator. Following this equation each quantity $I_i(x,y)$ has been obtained using two FFT. These routines can be used to evaluate a modal interaction matrix in the case of small rms aberration ($\ll$1 rad). Using a singular value decomposition algorithm we determined a modal least-square reconstruction matrix allowing us to obtain an estimate of the Zernike modes from the sensor signals.

[1] Sensor sensitivity refers to the ratio between the sensor signal rms and the incoming wavefront rms.

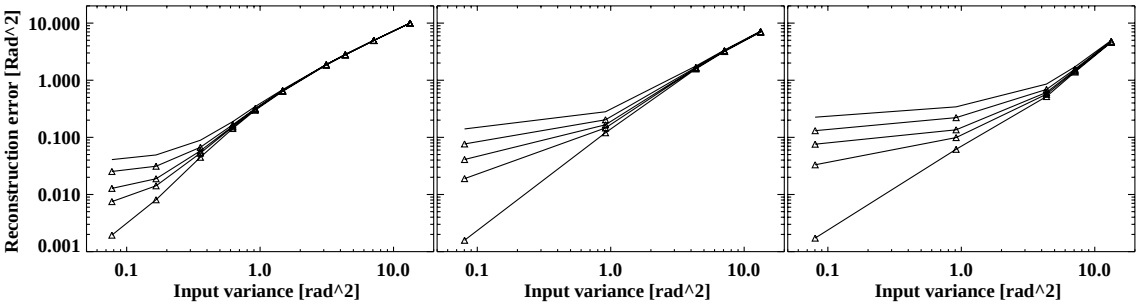

Fig. 3. Wavefront reconstruction error variance as a function of the corrected wavefront variance. The three plots (from left to right) refer to three angular tilt modulation amplitudes of zero, $\pm 1\lambda/D$ and $\pm 3\lambda/D$

4. A case study: MMT 6.5 m telescope

We consider below, as an example, the case of the 6.5 m MMT telescope (Lloyd-Hart et al. 2000). We simulate the operation of a PS having 16×16 sampling points arranged in a square grid on each of the four pupil images. The sensing wavelength is assumed 0.7 μm (R band) with $r_0 = 0.37$ m. The sampling time for the AO system is taken as 1 ms. The modal reconstructor used in this case allows the retrieval of 210 Zernike polynomials. However due to proper filtering of the singular values only 183 singular modes are taken into account. Finally the considered number of photons does not take into account any attenuation factor like optical elements transmission, CCD quantum efficiency and so on.

4.1. Reconstruction error $\sigma^2_{\rm rec}$

Firstly we quantify the wavefront reconstruction error $\sigma^2_{\rm rec}$ as a function of the variance of the partially corrected wavefront $\sigma^2_{\rm c}$, and of the number of received photons per sampling point per sampling time. The Zernike polynomial coefficients in the various sets of partially corrected wavefronts give a variance $\sigma^2_{\rm c}$ that ranges between 13 and 0.1 rad^2, going from very poor to very good wavefront correction. Finally we consider three different values of tilt modulation and so three different conditions of the sensor sensitivity. The reconstruction error variance $\sigma^2_{\rm rec}$ has been obtained as $\sigma^2_{\rm rec} = \sum_{i=2}^{N} < (z_i - \tilde{z}_i)^2 >$, where z_i and $\tilde{z}_i$ are the ith true and estimated Zernike coefficients respectively. The statistical average is obtained using 100 independent wavefront realizations. The results for $\sigma^2_{\rm rec}$ are shown in Fig. 3, where each plot corresponds to a different tilt modulation amplitude, namely zero modulation $\pm\lambda/D$, and $\pm 3\lambda/D$ (from left to right). Each plot contain five curves that represent $\sigma^2_{\rm rec}$ as a function of the variance $\sigma^2_{\rm c}$ for 10, 20, 50 and 100 photons per subaperture per integration time respectively (from top to bottom). The last curve is obtained when no photon noise is considered and quantifies the error due to sensor non linear effects. For comparison purposes the same simulation aimed at evaluating $\sigma^2_{\rm rec}$ for a SHS in the same cases of 10, 20, 50, 100 photons is performed. The obtained results are reported in Fig. 4. They agree with theoretical results

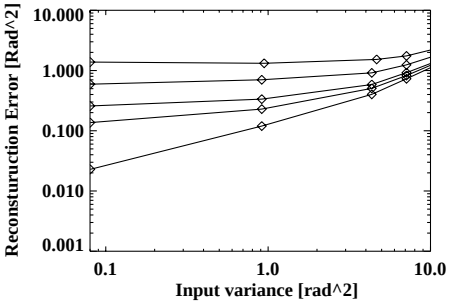

Fig. 4. Reconstruction error as a function of the input variance for a SHS

about SHS reconstruction error obtained by Rigaut and Gendron rigaut.

Comparison of Figs. 3 and 4 shows that when high $\sigma^2_{\rm c}$ values are considered a PS with no tilt modulation has higher $\sigma^2_{\rm rec}$ than SHS. When $\sigma^2_{\rm c}$ is lower than a certain threshold (4 rad^2 in our simulation), the use of tilt modulation allows a PS to achieve lower values of $\sigma^2_{\rm rec}$ than SHS. However the tilt modulation increases the $\sigma^2_{\rm rec}$ values achievable when low values of $\sigma^2_{\rm c}$ are considered. Finally it is interesting to note that simulation results suggest that to decrease PS reconstruction error when $\sigma^2_{\rm c}$ is higher than 4 rad^2 we have to increase the tilt modulation.

4.2. Limiting magnitude

Results of the previous subsection show that the limiting magnitude of a PS can be fainter than that for a SHS. The data obtained in the simulation and presented in Figs. 3 and 4 allows the limiting magnitude difference to be quantified. Using our data we obtain the relationship between $\sigma^2_{\rm rec}$ and the number of photons collected per subaperture per integration time $N_{\rm phot}$ at a given value of $\sigma^2_{\rm c}$. This is done by fitting the $\sigma^2_{\rm rec}$ data obtained at a certain $\sigma^2_{\rm c}$ with the relationship:

$$\sigma^2_{\rm rec} = A + B/N_{\rm phot} \qquad (6)$$

where A and B are parameters depending on $\sigma^2_{\rm c}$. In particular A accounts for non linear effect in the sensing process so that $\sigma^2_{\rm rec}$ is not zero when the number of received photons is infinite. Considering these relationships we determine the number of photons required to obtain

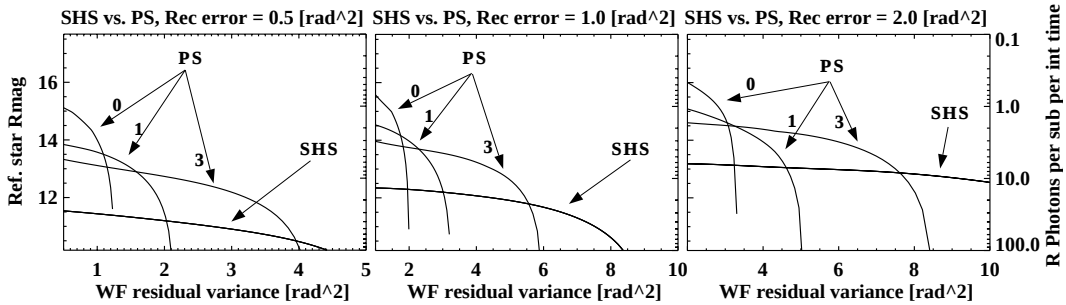

Fig. 5. Magnitude of the reference source needed to obtain a $\sigma^2_{\rm rec}$ value of 0.5, 1.0 and 2.0 rad^2 as a function of the corrected wavefront variance $\sigma^2_{\rm c}$ for PS and SHS. PS curves labelled 0, 1 and 3 refer to different tilt modulations cases of zero, $\pm 1\lambda/D$ and $\pm 3\lambda/D$

a certain value of $\sigma^2_{\rm rec}$ as a function of $\sigma^2_{\rm c}$. These photon numbers, $N_{\rm ps}$ and $N_{\rm shs}$, give the limiting magnitude comparison when a certain level of reconstruction error is fixed as a target. Results obtained are shown in Fig. 5. In this figure we consider three level of reconstruction error of 0.5, 1.0, and 2.0 rad^2 respectively. If we examine the case of 1.0 rad^2 residual. these results show that using zero tilt modulation the PS has a magnitude gain that is of about 3 mag with respect to a SHS. However, if the AO system can not achieve an overall phase error lower that 1.5 rad^2 the magnitude gain is strongly reduced or even nulled. In a partial correction regime, the tilt modulation allows to get again an important gain over the SHS. This is shown considering that using a tilt modulation of $1\lambda/D$ permits a 2 mag gain when the overall system phase error is lower than 2 rad^2 and decreases smoothly after this limit. Finally when using a modulation of about $3\lambda/D$ the gain is reduced to about 1.5 mag but this gain is retained until $\sigma^2_{\rm c}$ is lower than 5 rad^2. Similar results hold for the other values of $\sigma^2_{\rm rec}$ considered. This demonstrates the better behavior of PS with respect to SHS in terms of limiting magnitude even in partial correction AO systems.

5. Conclusion

A numerical simulation of PS and SHS in partial correction regime is performed. Our simulations show that in this regime the PS has better behavior then the SHS in terms of limiting magnitude. This better performance is obtained optimizing the tilt modulation amplitude depending on the partially corrected wavefront variance. Quantitatively results for MMT telescope for good seeing conditions show that reaching partial correction between 1–5 rad^2 allows to operate the PS with a limiting magnitude gain between 3.0−1.5 mag. In the considered case the tilt modulation is optimized between three different values namely zero, $\pm 1\lambda/D$, and $\pm 3\lambda/D$. Finally our analysis shows how the better PS performance, demonstrated in a diffraction limited correction regime (Ragazzoni & Farinato 1999) is retained using the tilt modulation, even with partial correction AO systems. This gain in limiting magnitude can be extremely important to solve or reduce the principal limitation of astronomical AO systems using natural star as reference sources, i.e. the limited sky-coverage.

Acknowledgements. The authors thank P. Salinari and R. Ragazzoni for useful comments and suggestions during the development of work reported in the present letter.

References

Babcock, H. M. 1953, PASP, 65, 229
Esposito, S., Bindi, N., Feeney, O., & Riccardi, A., Proc. Techno 1999 Conf., Sant' Agata, Italy
Esposito, S., Riccardi, A., & Feeney, O. 2000, Proc. SPIE, 4034, 184
Foucault, L. M. 1859, Ann. Obs. Imp. Paris, 5, 197
Gale Wilson, R. 1975, Appl. Opt., 14, 2286
Horwitz, B. A. 1994, Proc. SPIE, 2201, 496
Lloyd-Hart, M., Wildi, F. P. Martin, M., et al. 2000, Proc. SPIE, 4007, 167
Ragazzoni, R. 1996, J. Mod. Opt., 43, 289
Ragazzoni, R., & Farinato, J. 1999, A&A, 350, L23
Riccardi, A., Bindi, N., Ragazzoni, R., Esposito, S., & Stefanini, P. 1998, Proc. SPIE, 3353, 941
Riccardi, A., & Esposito, S., in preparation
Rigaut, F., & Gendron, E. 1992, A&A, 261, 677
Roddier, F. 1990, Appl. Opt., 29, 1402
Roddier, F., Northcott, M., & Graves, J. 1991, PASP, 103, 131
Roddier, N. 1990, Opt. Eng., 29, 1174